

# On the relation between the coronal line emission and the IR / X-ray emission in Seyfert galaxies<sup>★</sup>

M. Almudena Prieto<sup>1,2</sup>, A. M. Pérez García<sup>2†</sup> and J. M. Rodríguez Espinosa<sup>2</sup>

<sup>1</sup>*European Southern Observatory, Garching, Germany*

<sup>2</sup>*Instituto de Astrofísica de Canarias, E-38200, La Laguna (Tenerife), Spain*

Received.....; accepted.....

Accepted for publication in MNRAS

## ABSTRACT

The relation between the X-ray, the coronal line and the infrared (IR) emissions in a sample of the brightest known Seyfert galaxies is analysed. A close relationship between the absorption-corrected soft X-ray emission and both the mid-IR and the coronal line emission is found for the Seyfert type 2 objects in the sample. The coronal line and the X-ray emissions are both main tracers of the central activity, hence their relationship with the mid-IR emission points to nuclear energetic process as the main responsables of the heating of the circumnuclear dust. On the other hand, the above relations do not seem to hold for the Seyfert type 1 discussed in the sample, at least when the comparisons are done in a flux diagram. This is partially because of the reduced number of objects of this type analysed in this work and the fact that the measured soft X-ray emission in Seyfert 1s is systematically larger, by at least an order of magnitude, than that in the Seyfert 2 counterparts. Finally, the hard X-ray emission in the studied sample appears unrelated to either the mid-IR or the coronal line emission.

## 1 INTRODUCTION

Coronal lines arising in the spectra of active galactic nuclei (AGN) are unique tracers of the pure central power mechanism. These lines require ionization potentials (IP) beyond 50 eV and thus their study provide unique clues on the ultraviolet (UV) to soft X-ray region of

the AGN ionizing spectrum, this being a region difficult to probe with observations because of the heavy absorption at those energies. On the other hand, pure starbursts, where [OIV] 25.9  $\mu\text{m}$  is generally not present or very weak (Genzel et al. 1998; Lutz et al. 1998) do show photon energies below  $\sim 50$  eV.

In a previous paper (Prieto, Pérez García & Rodríguez Espinosa 2001), the coronal lines fluxes from [OIV]25.9  $\mu\text{m}$  and [NeV]14.5  $\mu\text{m}$  in the ISO (Infrared Space Observatory) spectra of a sample of the brightest known Seyfert galaxies are found to be directly related to the mid-IR continuum emission arising in these objects. Furthermore, Perez-Garcia & Rodríguez Espinosa (2001) report on the presence of two characteristic components in the IR continuum of Seyfert galaxies: a warm component peaking at 16  $\mu\text{m}$  and having a typical temperature in the 120-170 K range, and a cold component peaking at about 100  $\mu\text{m}$  and having a characteristic temperature in the 40-70 K range. In Prieto et al (2001), the coronal line emission is found to be strongly correlated with the warm-IR component but unrelated with the cold-IR one. Because of the nuclear origin of coronal lines, the above relations were interpreted as the mid-IR emission being due to dust heated mostly by processes associated with the AGN. The far-IR however is a different component, most probably due to dust heated by star forming regions in the disc of these galaxies and by the interstellar radiation field, and thus unrelated to the active nucleus.

In this paper, we explore the above relations further on the basis of available X-ray data for the galaxies in the sample. The reasoning behind is as follows. The IP of  $O^{2+}$  is about 50 eV and that of  $Ne^{3+}$  is roughly 100 eV, and thus a correlation between the [OIV] and [NeV] line fluxes and the soft X-ray emission might be anticipated. If, as argued in Prieto et al (2001), the mid-IR emission is due to dust mostly heated within the AGN nuclear region, a further relation between the mid-IR continuum emission and the soft X-ray emission may also be expected.

The present sample contains the brightest known Seyfert galaxies for which it was possible to obtain reliable measurements of the coronal lines [O IV] $\lambda$ 25.9 $\mu\text{m}$ , [Ne V] $\lambda$ 14.3 $\mu\text{m}$  using ISO. It includes seven Seyfert type 2 and four Seyfert type 1 among which are the prototype sources N1068, N4151 and Circinus. The ISO coronal line spectra of the sample are studied in Prieto & Viegas (2000); the mid-to-far IR continuum of the sample is studied in Pérez García & Rodríguez Espinosa (2001); the relationship between the IR continuum and the coronal line emission is discussed in Prieto et al. (2001).

## 2 OBSERVATIONAL DATA

### *Coronal line data*

The sample of Seyfert galaxies used in this work was originally presented in Prieto & Viegas (2000). All the galaxies were observed with the ISOSWS (ISO-Short Wavelength Spectrometer) at the wavelengths of the coronal lines [O IV] $\lambda$ 25.9 $\mu$ m, [Ne V] $\lambda$ 14.3 $\mu$ m, [Mg VIII] $\lambda$ 3.02 $\mu$ m and [Si IX] $\lambda$ 2.58 $\mu$ m. Regardless of the Seyfert type, the strongest coronal lines found in the ISO spectra of these objects are the [OIV] and [NeV] lines (cf. Table 1 in Prieto & Viegas). In the present analysis, only the emission from these two lines is considered. The integrated fluxes correspond to the ISO-SWS aperture of 20x33 arcsecs.

### *Mid-IR continuum data*

Continuum fluxes at 16, 25, 60, 90, 120, 135, 180 and 200  $\mu$ m were measured with ISOPHT (ISO-Photopolarimeter) for all the galaxies in the sample by Pérez García & Rodríguez Espinosa (2001). Only the fluxes at 16, 25 and 60 $\mu$ m are considered in this work. These data are complemented with ground-based data at 10 $\mu$ m existing for all the sources. The latter are taken from compilations by Contini, Prieto & Viegas (1998), Edelson (1978), Rieke & Lebofsky (1978), Edelson, Malkan & Rieke (1987) and Maiolino et al. (1998). The 10 $\mu$ m fluxes correspond to integrated fluxes within an aperture between 5 and 8.5 arcsec. The 16 and 25 $\mu$ m values correspond to integrated fluxes within a 120 or 180 arcsec aperture, depending on the size of the objects. The 60  $\mu$ m data were acquired with the C100 detector consisting of a 3x3 panoramic pixel array, each pixel projecting on 45 arcsec on the sky.

### *Soft X-ray data*

For most of the galaxies, the soft X-ray emission, namely the 0.2-2.4 keV region, is primarily taken from the *ROSAT* PSPC (Position Sensitive Proportional Counter). After searching in the literature, a large diversity in the way soft X-ray fluxes were derived and reported was found. As soft X-ray fluxes are largely dependent on the absorption correction applied, to ensure homogeneity, whenever PSPC pointing observations were available, X-ray fluxes were derived by ourselves. In this case and due to the poor spectral resolution of the *ROSAT* PSPC, the general approach is to fit a single power-law model corrected by absorption to the PSPC spectra. We note that among the various parameters derived from the fit, integrated fluxes are the least dependent on the model adopted. Free parameters in the fit were the H column density N(H), the power-law spectral index and the normalization factor. In all cases, statistically acceptable fits were obtained, with all the fit parameters

being derived within reasonable constraints. In those cases in which the H column density was found lower than the corresponding Galactic value, the latter was used as a fixed parameter in the fit and the integrated X-ray flux derived accordingly. The X-ray fluxes, their 1 sigma uncertainty and the  $N(\text{H})$  are given in Table 1. Details of the fit for individual sources are given in the caption to Table 1.

In the case of sources with known complex spectrum and/or morphology, absorption-corrected fluxes were taken from the literature. References for those and the adopted  $N(\text{H})$  are given in the caption to Table 1. In these cases, the error associated with the X-ray flux represents the amplitude of the flux variation between different measurements found in the literature. Besides, some of the objects in the sample are known to be variable, e.g. NGC 4151, NGC 5548. We expect to account for this effect by including in the errors the maximum range of fluxes reported in the literature.

#### *Hard X-ray data*

Absorption-corrected fluxes in the 2-10 keV, giving preference to *ASCA* or *BESPOSAX* data, were taken from the literature for all the objects. In general, when several values were found, the average was used and the associated error reflects the amplitude of the variation. Fluxes and the sources for these data are also given in Table 1. The sample includes three known Compton thick sources: NGC 1068, Mrk 533 and Circinus. In these cases, the reported hard X-ray fluxes may be subjected to large uncertainties and should be taken with caution. The large error bars associated to these sources accounts for the large spread in values reported by different authors and that on the model used.

### **3 RESULTS**

Fig. 1 compares the absorption-corrected soft X-ray emission with the [OIV] and [NeV] coronal line fluxes respectively, as well as with the 10, 16, 25 and  $60\mu\text{m}$  continuum emission for the galaxies in the sample. The comparison with the respective warm- and cold- IR emission as defined in Pérez García & Rodríguez Espinosa (2001, see also section 1) is also shown in the last row.

Two facts are readily seen. First, there is a kind of separation in behavior between the two Seyfert types; secondly, the soft X-ray fluxes correlate rather well with the coronal line fluxes (Figure 1, first row), particularly with [OIV], the line with better signal-to-noise in the ISO spectra, and with the  $10\mu\text{m}$  continuum emission fluxes (Fig.1, second row). The

correlation also holds when the soft X-ray emission is compared with the progressively colder IR fluxes, but degrades when ISO fluxes from  $60 \mu m$  on are considered (Fig. 1, third row; to avoid redundancy the comparisons with fluxes above  $60 \mu m$  are not shown). Similarly, as expected based on the above, a positive trend appears when the comparison is done with the warm IR flux whereas no correlation is seen with the cold IR fluxes (Fig. 1, last row).

The intermediate Seyfert type 1.5 galaxy, NGC 4151, follows the trend defined by the Seyfert 2 type objects. However, the four Seyfert 1 objects in the sample, NGC 5548, NGC 5033, Mrk 335 and Mrk 817, markedly depart from the Seyfert 2 behavior. Indeed, the soft X-ray emission in these objects is larger by more than an order of magnitude than that measured in the Seyfert 2s. The trends described above contrast with the pure scatter diagram that arises when the comparison is done with the absorption-corrected hard X-ray fluxes regardless of Seyfert type (Fig. 2). In this case, both the coronal line emission and the mid-IR emission appear unrelated to the hard X-ray emission.

For comparison purposes, Fig. 3 shows the same comparisons as in Fig. 1 but in luminosity plots. As expected, the trends seen in the flux diagrams show are also seen in the luminosity diagrams. Note however that no correlation is present between the soft X-rays and the  $60 \mu m$  luminosities, as already revealed in the flux diagram. Also, the Seyfert 1 galaxies show larger X-ray luminosities than their Seyfert 2 counterparts for the same IR luminosity. The few Seyfert 1s in the sample appear rather scattered in the luminosity diagrams; there is a hint for a positive trend in the comparison with the [OIV] coronal line emission, yet the reduced number of S1s in the sample prevents further conclusion.

To the best of our knowledge, only Penston et al. (1984) conducted a similar study addressing the possible relationship between coronal line and X-ray emissions in a large sample of AGN. These authors found a pure scatter diagram when comparing in their case the optical [FeX]  $6374 \text{ \AA}$  coronal line flux and the 2-10 keV flux. This result is therefore fully in agreement with the results presented here. No comparisons involving soft X-ray and coronal line emissions are reported in the literature and thus, the results presented here are unique on that respect.

Many authors, however, have addressed the study of the soft X-ray to IR relation in Seyfert galaxies on the basis of much larger samples than the one used here. Results from those works are briefly compared with our results in the following.

In general, there is broad agreement on the lack of correlation between the X-ray and the far-IR *IRAS* luminosities in Seyfert galaxies (e.g. David, Jones & Forman 1992; Green,

Anderson & Ward 1992); indeed a degradation of the X-ray/ IR correlation with increasing IR wavelength is postulated by Giuricin, Mardirossian & Mezzetti (1995) and Danese et al. (1992). This conclusion is thus in agreement with the results presented here.

Focusing on the mid-IR vs soft X-ray relationship, there is a larger diversity in the reported results. Green et al. (1992) report of no correlation in their sample, regardless of the Seyfert type when comparing the *IRAS* 12  $\mu\text{m}$  and the Einstein 0.5-4.5 keV luminosities whereas Giuricin et al.(1995) report on a weak positive correlation with the 10  $\mu\text{m}$  emission in Seyfert 2 objects only; Rush et al (1996) find a tight correlations between the *ROSAT* 0.1-2.4 keV and the 12  $\mu\text{m}$  *IRAS* luminosity for both Seyfert types but with Seyfert 1s having relatively more soft X-ray emission than Seyfert 2s for the same mid-IR luminosity by 1-2 orders of magnitude. This shift in X-ray luminosities is also found by Green et al (1992). We find clear positive trends for the Seyfert 2 objects when comparing their soft X-rays with either the coronal line or the 10–25  $\mu\text{m}$  emissions. A similar trend is not seen in the Seyfert 1s although this may be due to the small number of objects of that class in the sample. As expected, the S1s in the sample show X-ray luminosities larger by 1-2 order of magnitude than those in S2s, which make them depart from the Seyfert 2 trend. Thus, our results are supported by those found by Rush et al (1996). We believe that part of the reason for the discrepancy with the results of Green et al and Giuricin et al. resides on the much harder X-ray band pass used by those authors, 0.5- 4.5 keV. This band might include an important contribution from the central non-thermal AGN emission, which may be smearing out the underlying mid-IR to soft X-ray relation, readily seen when considering the softer 0.1-2.4 keV region.

Moving to the hard X-rays, Giuricin et al. (1995) find the 2-10 keV emission weakly related to the 10  $\mu\text{m}$  emission in their sample. Interestingly, the authors also point out that the apparent correlation becomes weaker and weaker as they restrict themselves to the nearer objects. As indicated above, Penston et al (1984) find no correlation between the coronal line [FeX] flux and the hard X-ray fluxes. We find no apparent trend between the hard X-ray emission and either the coronal line or the IR continuum emissions. Although the sample is small, we note that the observed scatter in the diagrams extends over five orders of magnitude in the X-rays in a sample of relatively nearby objects - the farthest object being less than 200 Mpc distance. Part, but not all, of the scatter may be introduced by the three Compton-thick sources in the sample. In any case, the lack of correlation appears to

point into the direction indicated by Guiricin et al., namely, the progressive weakness of the relation for the nearer objects in their sample.

#### 4 DISCUSSION

The [OIV] and [NeV] coronal lines discussed herein imply ionization potential of 50 eV and 100 eV respectively for the corresponding ions to be produced. Regardless of weather photoionization and/or shocks, the strength of these line should depend, at least partially, on the available energy budget beyond 50 eV. Considering that the energy required to produce those high ionization species is very close to the soft X-ray energies analysed here, a trend between the coronal line emission and the soft X-ray emission is to be expected. This is precisely what is observed for the Seyfert 2 objects in this sample.

The soft X-ray emission in the Seyfert 2 objects is also related to the mid-IR emission of these galaxies. The relationship, however, is stronger when the comparison is made with the ground-based  $10\mu m$  fluxes, which is somehow expected if one considers that the apertures used in that case are about or smaller than 5-8 arcsecs. A progressive degradation of that correlation is observed with increasing IR wavelength. On the other hand, Prieto et al. (2001) find the ISO mid-IR emission closely related to the coronal line emission arising in the nucleus of these galaxies. The strongest relation is seen as well with the  $10\mu m$  emission and degrades progressively with increasing IR wavelength. Putting all together, the general trend of the mid-IR emission when compared with either the X-ray or the coronal emission points out the central AGN environment and the energetic process associated with it as the dominant heating source of the circumnuclear dust. Some dispersion in the above relations is expected, however, as a result of the contribution from other sources unrelated with the active region. For example, we may expect an additional heating contribution by circumnuclear star-forming regions, particularly at the IR wavelengths caused by the large ISO apertures. In the X-rays, star formation activity, X-ray binaries and gas halos can also contribute to the soft X-ray emission. Yet, considering the unique link between coronal line emission and AGN activity, the good correlations found indicate that those contributions are at least not dominant.

The few Seyfert 1 galaxies in the sample present soft X-ray emissions larger by at least an order of magnitude than those measured in the Seyfert 2 objects. This difference, already known from previous studies based on much larger samples of Seyfert galaxies (e.g. Green

et al. 1992; Rush et al 1996), make them already depart from the overall trend shown by the Seyfert 2s in both the coronal-line- and versus the soft X-ray and the mid-IR versus soft X-ray relations. None of the above relations seem to apply to the few S1s in this sample; yet, some hint of a positive trend in the luminosity plot, in particular when comparing the [OIV] and soft X-ray emissions, is however apparent. Clearly, any confirmation of the above results requires the analysis of a much large number of S1 objects. We would, however, like to note the following. Within the framework of the unified Seyfert schemes, the observed larger X-ray flux in Seyfert 1s indicates our preferential line of sight to the central source of these objects, that being otherwise suppressed or much absorbed in Seyfert 2s as a result of the presence of a central obscuring structure -the putative disc/torus. A lack of correlation in S1s could indicate that the dominant and perhaps anisotropic central X-ray emission in these objects prevents us for seeing the underlying, somehow mandatory, relation between the coronal line and the soft X-ray emission. In Seyfert 2, being the primary central emission absorbed, the correlation of the coronal emission with the central reprocessed soft X-ray emission can readily be seen. It is worth mentioning that the only intermediate Seyfert type (1.5) in the sample, NGC 4151, fits perfectly within the Seyfert 2 trend in all the diagrams.

Coronal lines are formed in an intermediate region between the broad and the narrow line region. These lines are seen in both Seyfert type with similar strengths. Their correlation with the mid-IR emission regardless of the Seyfert type, indicates that in both cases the emission arise most likely from the outer regions of the torus. The fact that both Seyfert type also span similar ranges of mid-IR luminosities lead Rush et al (1996) to similar conclusion. Because the coronal line emission in S2s further correlates with the soft X-rays, both emissions should be co-spatial and therefore soft X-rays may well be produced at the outer regions of the torus.

One of the most popular scenarios attempting to explain the soft X-ray emission in Seyfert 2 galaxies is the electron-scattering of nuclear X-rays into our line of sight (Miller, Goodrich & Matthews 1991). An alternative scenario is the case in which the soft X-rays are bremsstrahlung emission from hot gas heated by shocks induced by the central radiation pressure (Viegas & Contini 1994, Morse et al. 1996; Contini & Viegas 2001). The modeling of the spectral energy distribution of Seyfert galaxies by Contini et al. (1998 and references therein) shows that the re-emission by dust is closely related to bremsstrahlung from hot gas in the vicinity of the nucleus. The temperature of the gas and that of the grains are found closely related to each other. In these models, which account for the combined effect of photoionization and shocks, the soft X-rays are mainly emitted by hot gas in the immediate



post shock region. Mutual heating between the dust and the gas leads to the corresponding emission by dust in the near- and mid-IR. The observed relationship between the mid-IR emission and the soft X-ray emission in the Seyfert 2 objects analysed here provide support to this scenario. The comparison of the models predictions with the present correlations will be discussed in detail in Viegas et al (in preparation).

Regarding the hard X-rays, there is an apparent lack of correlation between the hard X-ray emission and either the coronal line (in agreement with Penston et al. 1974) or the IR continuum (in partial agreement with Giuricin et al. 1996 who only find a weak correlation). The result may be surprising, considering that with the exception of the Compton thick sources the measured hard X-rays are mostly primary AGN emission and therefore a link with other AGN-related emission processes may be expected. On the other hand, we first note that the energies required to produce the high ionization coronal lines are well below 2 keV; and secondly, the heating of the dust with energies above 2 keV would either destroy the dust or shift the peak of the emission to higher IR frequencies. In the latter case a positive trend between hard X-ray and near IR emissions may be expected and indeed that seems to be observed, at least among Seyfert 1 galaxies (e.g. Kotilainen et al 1992). Clearly, the present analysis on a much large sample of Seyfert galaxies could set more firm conclusions on the results discussed.

## REFERENCES

- Bassani, I., Dadina, M., Maiolino, R., Salvati, M., Risaliti, G., della Ceca, R., Matt, G., Zamorani, G., 1999, ApJS 121, 473  
 Contini, M., Prieto, M.A., & Viegas, S.M. 1999 ApJ, 505, 621  
 Contini & Viegas 2001, ApJS 132, 211  
 Danese, L., Zitelli, V., Granato, G. L., Wade, R., de Zotti, G., Mandolesi, N., 1992, ApJ 399, 38  
 Davies, R., Ward, M. & Sugai, H. 2000, ApJ 535, 735  
 David, L.P., Jones, C. & Forman W. 1992, ApJ 388, 82  
 Edelson, R.A., Malkan, M.A. & Rieke, G.H. 1987, ApJ, 321, 233  
 Edelson, R.A. 1978, ApJ, 226, 550  
 George, I. M., Turner, T. J., Netzer, Hagai, Nandra, K., Mushotzky, R. F., Yaqoob, T., 1998, ApJS 114, 33  
 Genzel, R.; Lutz, D.; Sturm, E.; Egami, E.; Kunze, D.; Moorwood, A. F. M.; Rigopoulou, D.; Spoon, H. W. W.; Sternberg, A.; Tacconi-Garman, L. E.; Tacconi, L.; Thatte, N., 1998, ApJ, 498, 579  
 Giuricin, G., Mardirossian, F. & Mezzetti, M. 1995, ApJ 446, 550  
 Green, P. J., Anderson S.F. & Ward, M. 1992, MNRAS 254, 30  
 Guainazzi, M., Matt, G., Antonelli, L. A., Bassani, L., Fabian, A. C., Maiolino, R., Marconi, A., Fiore, F., Iwasawa, K., Piro, L., 1999, MNRAS 310, 10  
 Iwasawa, K., Fabian, A. C., Nandra, K., 1999, MNRAS 307, 611

- Kotilainen, J., Ward, M. Boisson, C. DePoy, & Smith M. G. 1992, MNRAS 256, 149
- Lutz, D.; Kunze, D.; Spoon, H. W. W.; Thornley, M. D., 1998, A&A, 333, L75
- Maiolino, R., Krabbe, A., Thatte, N., Genzel, R., 1998, ApJ 493, 650
- Matt, G., Guainazzi, M., Maiolino, R., Molendi, S., Perola, G. C., Antonelli, L. A., Bassani, L., Brandt, W. N., Fabian, A. C., Fiore, F., Iwasawa, K., Malaguti, G., Marconi, A., Poutanen, J., 1999, A&A 341, L39
- Miller, J.S, Goodrich, R. W., Matthews W.G., 1991, ApJ 378, 47
- Morse, J, Raymond, J, Wilson A., 1996, PASP 108, 426
- Nandra, K., Fabian, A. C., George, I. M., Branduardi-Raymont, G., Lawrence, A., Mason, K. O., McHardy, I. M., Pounds, K. A., Stewart, G. C., Ward, M. J., Warwick, R. S., 1993, MNRAS 260, 504
- Pérez García, A.M, Rodríguez Espinosa, J.M., 2001, ApJ, 557, 39
- Polleta, M., Bassani, L., Malaguti, G. Palumbo, G. & Caroli, E., 1996, ApJS106, 399
- Prieto, M.A. & Viegas, S. 2000, ApJ 532, 238
- Prieto, M.A., Pérez García, A.M., Rodríguez Espinosa, J.M., 2001. A&A, 377, 60
- Penston, M., Fosbury, R. A. E., Boksenberg, A., Ward, M. J., Wilson, A. S., 1984, MNRAS 208, 347
- Rieke, G.H., Lebofsky, M.J., 1978, ApJ, 222, 49
- Rush, B., Malkan, M. Fink, H. & Voges, W., 1996, ApJ 471, 190
- Wang, J., Heckman, T. M., Weaver, K. A., Armus, L., 1997, ApJ 474, 659
- Warwick, R. S.; Smith, D. A.; Yaqoob, T.; Edelson, R.; Johnson, W. N.; Reichert, G. A.; Clavel, J.; Magdziarz, P.; Peterson, B. M.; Zdziarski, A. A., 1996, ApJ, 470, 349
- Weaver, K. A., Mushotzky, R. F., Arnaud, K. A., Serlemitsos, P. J., Marshall, F. E., Petre, R., Jahoda, K. M., Smale, A. P., Netzer, H., 1994, ApJ 423, 621
- iegas, S. & Contini, M., 1994, ApJ 428, 113

Object	Type	v Km s <sup>-1</sup>	F(0.2-2.4keV) erg cm <sup>-2</sup> s <sup>-1</sup>	errF(0.2-2.4keV)	N(H) 10 <sup>21</sup> cm <sup>-2</sup>	F(2-10 keV) erg cm <sup>-2</sup> s <sup>-1</sup>	errF(2-10 keV)
NGC5548	1	5152	2.4×10 <sup>-11</sup>	1.5×10 <sup>-11</sup>	0.16±0.01	6.7×10 <sup>-10</sup>	1.1×10 <sup>-10</sup>
NGC5929	2	2490	2.49×10 <sup>-13</sup>	1.3×10 <sup>-14</sup>	0.58±0.15	≤7.9×10 <sup>-12</sup>	
Mrk817	1	9436	4.04×10 <sup>-12</sup>	2.3×10 <sup>-13</sup>	0.06±0.03		
Mrk335	1	7688	7.00×10 <sup>-11</sup>	4.0×10 <sup>-12</sup>	0.41 fix	1.2×10 <sup>-11</sup>	4.0×10 <sup>-11</sup>
Mrk266	2	8360	9.80×10 <sup>-13</sup>	9.0×10 <sup>-13</sup>	0.6±0.27	≤8.0×10 <sup>-13</sup>	
Mrk533	2	8670	3.40×10 <sup>-13</sup>		1.8fix	5.0×10 <sup>-13</sup>	
Mrk334	2	6582	≤2.80×10 <sup>-13</sup>		0.44 fix	≤1.3×10 <sup>-11</sup>	
NGC1144	2	8648	1.10×10 <sup>-13</sup>	8.0×10 <sup>-14</sup>	0.5 fix	≤1.2×10 <sup>-11</sup>	
NGC5033	1	876	8.0×10 <sup>-12</sup>	6.0×10 <sup>-12</sup>	0.25±0.07	5.5×10 <sup>-12</sup>	
CIRCINUS	2	436	1.60×10 <sup>-11</sup>	2.0×10 <sup>-12</sup>	0.5±0.04	7.4×10 <sup>-11</sup>	1.0×10 <sup>-10</sup>
NGC1068	2	1140	5.60×10 <sup>-11</sup>	2.4×10 <sup>-11</sup>	2.5±0.7	3.5×10 <sup>-12</sup>	8.0×10 <sup>-12</sup>
NCG4151	1.5	980	4.00×10 <sup>-12</sup>	1.0×10 <sup>-12</sup>	~ 49 ± 2	2.7×10 <sup>-10</sup>	1.0×10 <sup>-10</sup>

**Table 1.** Mrk 335: Soft X-ray flux from Rush et al (1996) corrected by the Galactic absorption. The absorption-corrected hard X-ray flux from George et al (1998). NGC 5033: average soft X-ray flux from Polleta et al (1996) corrected by the Galactic absorption. Absorption-corrected hard X-ray flux is from Bassani et al (1999). Mrk 533: Soft X-ray flux from Polleta et al (1996) corrected by the Galactic absorption. The *ROSAT*/PSPC pointing spectrum is very noisy: we derive the same flux value from a single power-law fit to the PSPC spectrum assuming spectral index  $\alpha = -1$  and Galactic absorption. Absorption-corrected hard X-ray flux from Bassani et al. (1999). NGC 1144: Soft X-ray flux derived in this work from a power-law fit to the *ROSAT*/PSPC spectrum and Galactic absorption; error represents one sigma uncertainty in the fit. The hard X-ray flux is an upper limit from Polleta et al (1996). NGC 5929: Soft X-ray flux derived in this work from an absorbed power-law fit to the *ROSAT*/PSPC spectrum; error represents one sigma uncertainty. Hard X-ray is an upper limit from Polleta et al (1996). Mrk 266: Average soft X-ray flux from Wang et al. (1997) derived from a range of N(H) values. Only the flux from the South component –identified as the AGN component by Davies et al (2000) – is considered. Hard X-ray flux from Polleta et al (1996). NGC 1068: absorption corrected soft X-ray flux from Guainazzi et al (1998); the error accounts for Polleta et al (1996) value corrected by the Galactic absorption. Absorption-corrected hard X-ray flux from Bassani et al (1999); the error bar accounts for the absorption-corrected flux from Guainazzi et al (1998). NGC 4151: absorption-corrected soft X-ray flux from Warwick et al (1996) and Weaver et al (1994) (average value). Absorption-corrected hard X-ray flux from Warwick et al (1996) and George et al (1998) (average value). Circinus: absorption corrected soft X-ray flux from Guainazzi et al (1998); error accounts for Polleta et al (1996) value corrected by the Galactic absorption. Absorption-corrected hard X-ray flux from Guainazzi et al (1998); error accounts for absorption-corrected flux from Matt et al (1999). Mrk 334: Soft X-ray flux derived in this work from *ROSAT*/PSPC survey data assuming a power-law with photon index -2 and Galactic absorption. The hard X-ray flux is an upper limit from Polleta et al (1996). Mrk 817: Soft X-ray flux derived in this work from a single power-law fit to the *ROSAT*/PSPC spectrum corrected by Galactic absorption; error represents one sigma uncertainty. No hard X-ray data available. NGC 5548: Absorption-corrected soft X-ray flux from Iwasawa et al (1999) and Nandra et al (1993) (average value). Absorption-corrected hard X-ray flux from George et al (1998).

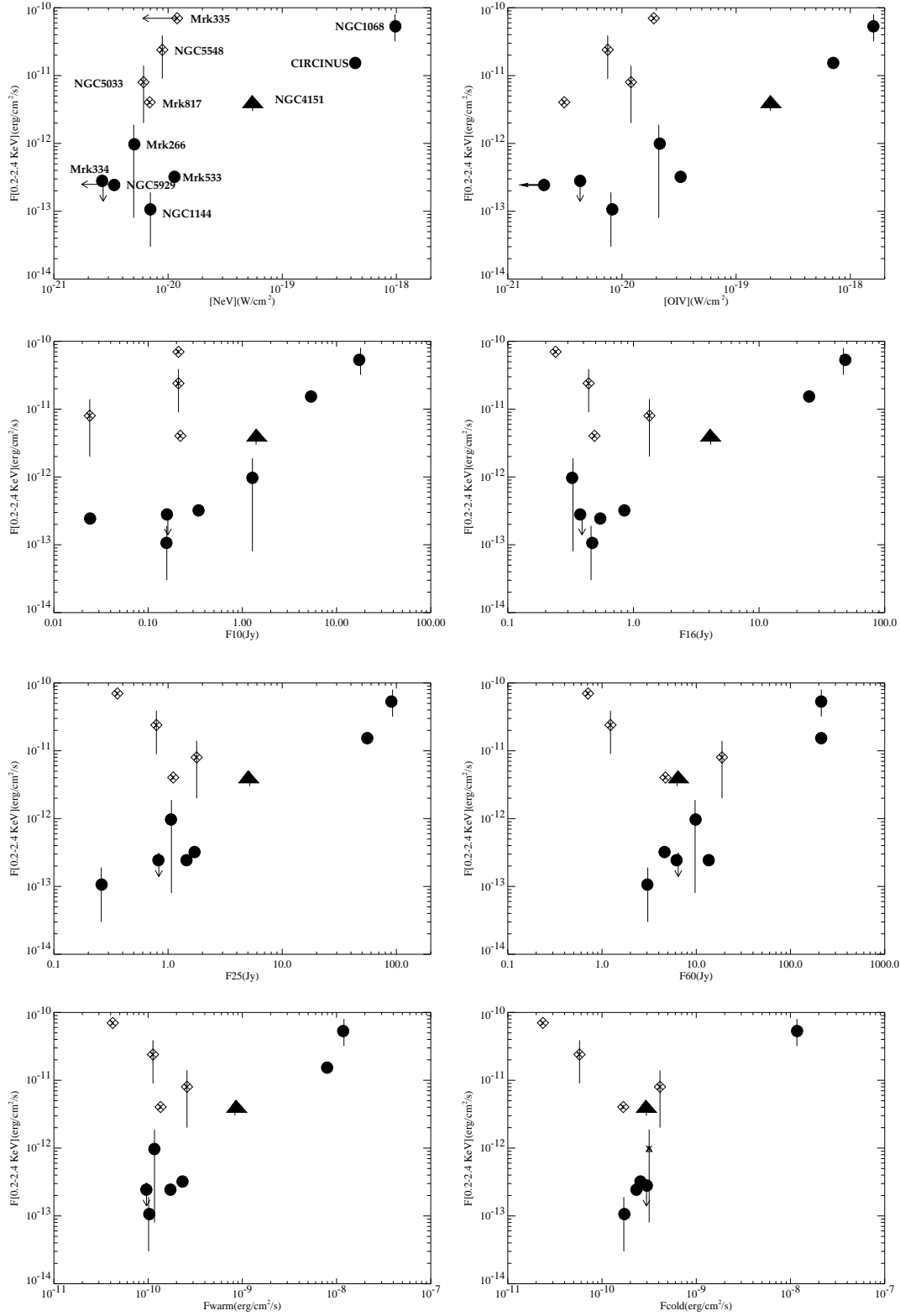


**Figure 1.** The absorption-corrected soft X-ray emission for the galaxies in the sample is compared with the [OIV] and [NeV] coronal line fluxes (first row); with the 10, 16, 25 and  $60\mu\text{m}$  continuum emission (second and third rows); and with their respective warm- and cold- IR emission as defined in Pérez García & Rodríguez Espinosa (2001) (last row). Seyfert 1 galaxies are represented by open diamonds, and the Seyfert 2 galaxies are marked with filled circles. The intermediate type, NGC 4151 is marked with a triangle.

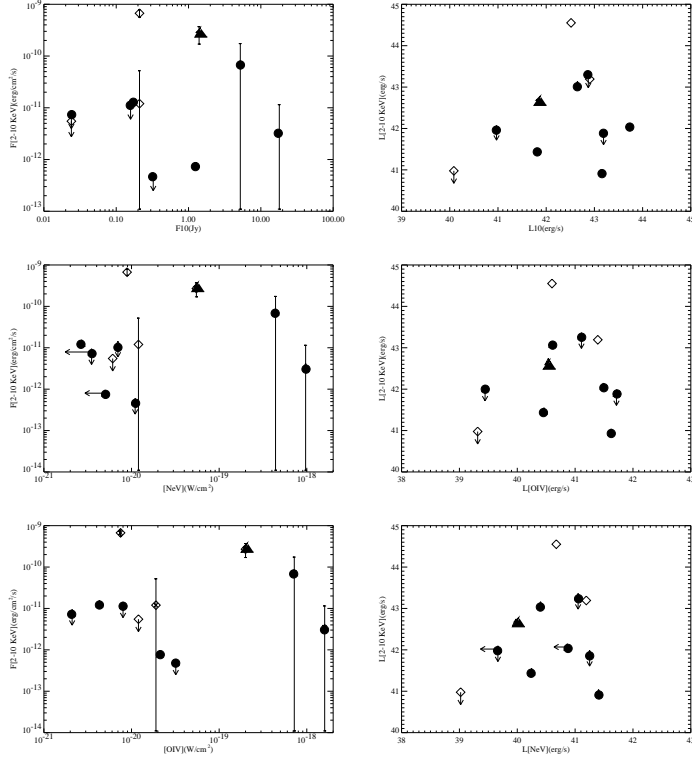


**Figure 2.** The absorption-corrected hard X-ray emission for the galaxies in the sample is compared with the 10  $\mu$ m emission and with [OIV] and [NeV] coronal line emission. Fluxes are compared in the left column, luminosities in the right column. Symbols are as in Fig. 1. Notes on individual galaxies are given in the caption to Table 1.

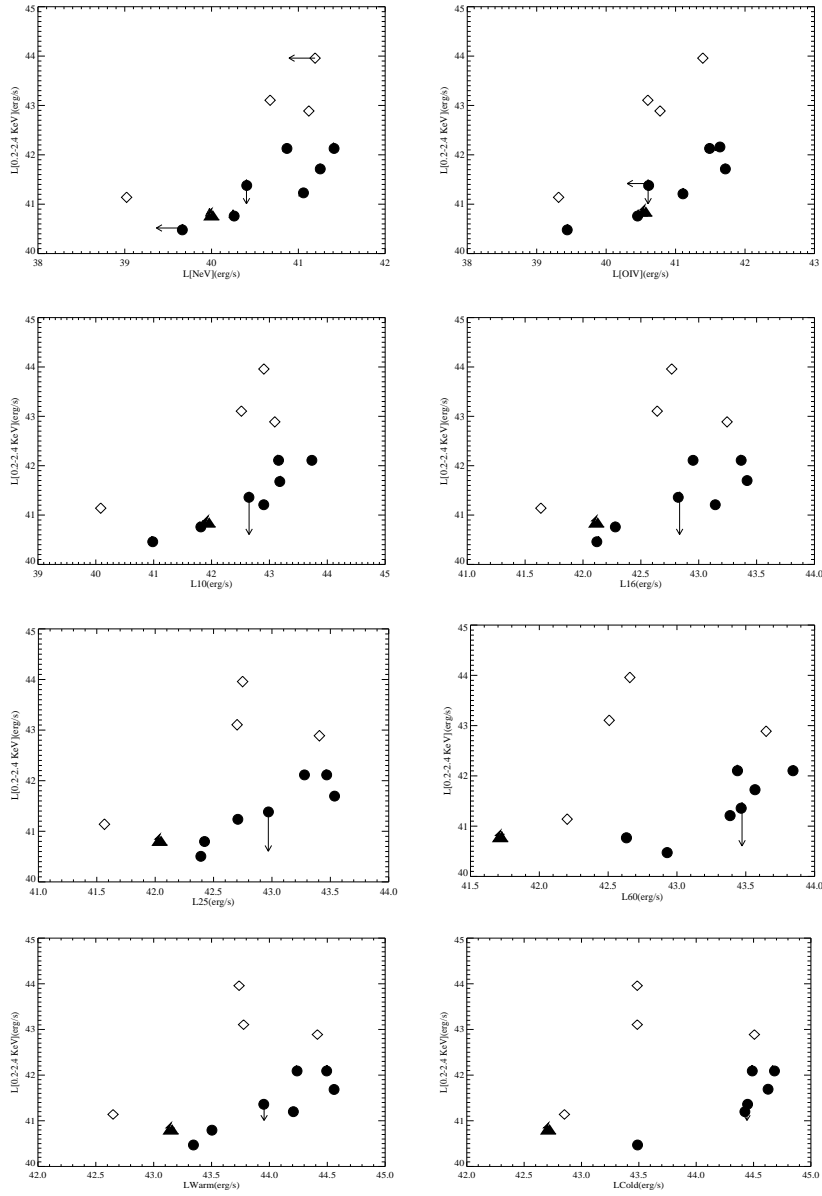


**Figure 3.** As in Figure 1 but in luminosity plots, Symbols as in Fig. 1.